



**Localization of pairs in one-dimensional quasicrystals with power-law hopping**G. A. Domínguez-Castro  and R. Paredes\**Instituto de Física, Universidad Nacional Autónoma de México, Apartado Postal 20-364, México D.F. 01000, Mexico* (Received 28 March 2022; revised 30 August 2022; accepted 5 October 2022; published 26 October 2022)

Pair localization in one-dimensional quasicrystals with nearest-neighbor hopping is independent of whether short-range interactions are repulsive or attractive. We numerically demonstrate that this symmetry is broken when the hopping follows a power law  $1/r^\alpha$ . In particular, for repulsively bound states, we find that the critical quasiperiodicity that signals the transition to localization is always bounded by the standard Aubry-André critical point, whereas attractively bound dimers get localized at larger quasiperiodic modulations as the range of the hopping increases. Extensive numerical calculations establish the contrasting nature of the pair energy gap for repulsive and attractive interactions, as well as the behavior of the algebraic localization of the pairs as a function of quasiperiodicity, interaction strength, and power-law hops. The results here discussed are of direct relevance to the study of the quantum dynamics of systems with power-law couplings.

DOI: [10.1103/PhysRevB.106.134208](https://doi.org/10.1103/PhysRevB.106.134208)**I. INTRODUCTION**

Quasicrystals are intriguing structures that are characterized by having long-range order without spatial periodicity. Such exotic states of matter constitute intermediate cases between disordered and periodic systems. Due to their particular spatial arrangement, the localization of individual particles in one-dimensional quasicrystals has been explored both theoretically [1–8] and experimentally [9–11]. In particular, considerable attention has been given to the celebrated Aubry-André (AA) model [1,12,13]. In this model, quasiperiodicity emerges by superimposing two lattices with incommensurate periods [14], and particles hop through nearest-neighbor sites only. To enrich the localization problem in the AA model, one can replace the nearest-neighbor tunneling with a hopping the amplitude of which follows a power law. This modification is of particular interest since power-law interactions arise in many important systems [15], for instance, polar molecules [16–18], Rydberg atoms [19,20], trapped ions [21–23], and atoms in photonic crystal waveguides [24], among others. Intriguing results, such as multifractal states [25,26] and algebraic localization [27], arise as a consequence of the interplay between quasiperiodicity and power-law hops.

One of the fundamental questions in localization theory, which has sparked intense debate [28–37], is the fate of the Anderson transition in the presence of interactions at finite particle density. This subject, called the many-body localization problem [38], faces significant computational and experimental challenges. From the numerical side, exact diagonalization methods are restricted to small-size systems due to the exponential growth of the Hilbert space, and tensor network algorithms [39–41] allow one to simulate the dynamics of larger systems, but up to times limited by the amount of entanglement in the many-body system. On the other hand,

experiments are restricted to several hundred tunneling times due to the coupling with the external environment [42–45]. This limitation makes it difficult to extrapolate the results to the infinite time limit, where a slow decay regime can be straightforwardly distinguished from the peculiar frozen dynamics of many-body localization.

Because of the complexity of the many-body localization problem, it is reasonable to focus our attention on the localization properties of few-body systems. Although the collective behavior of matter indeed demands the participation of a large conglomerate of entities, the physics of two or few interacting particles can contain the essence from which one can understand the properties of a many-body system. In fact, despite its apparent simplicity, the pair localization problem already exhibits rich physics, for instance, the enhancement of the pair localization length [46–49], the interaction effect on the dimer localization [50–57], the presence or absence of mobility edges [58,59], the fractal character of the two-body spectrum [60], and exotic dynamical regimes [61], among others. Furthermore, due to the high precision and tunability achieved on several quantum simulation platforms, observing few-body phenomena is within reach of current experiments [62–64].

In this paper, we study a fundamental two-body model that incorporates the essential ingredients discussed above: short-range interactions, quasiperiodic potential, and power-law hopping. To the best of our knowledge, there is no study that discusses the interplay of the three former elements on the pair localization transition. We numerically demonstrate that, in stark contrast with quasicrystals with nearest-neighbor hops [46,48,50,52,57], the mirror symmetry of the critical quasiperiodicity, where localization occurs, breaks when the hopping range is increased. That is, its value depends on whether the interactions are attractive or repulsive. Our calculations show that the critical quasiperiodic modulation for repulsively bound states is always bounded by the usual Aubry-André transition point [1,14], whereas attractively

\*rosario@fisica.unam.mx

dimers localize at larger quasiperiodic modulations when the range of the hopping increases. Through robust numerical calculations, we study the pair energy gap and the algebraic decay of both repulsively and attractively bound dimers. Furthermore, we introduce an effective Hamiltonian that describes the two-body system within the tightly bound regime and compare its predictions with the full two-body problem. The results here discussed go beyond previous findings [48,50,53], in the sense that they explore the consequences of the range of the hopping on the two-body localization transition. Furthermore, they are of main relevance for current studies on the quantum dynamics of bound states in optical lattices [61,65–67].

The paper is organized as follows. In Sec. II we introduce the model considered and develop the Green's function formalism used to address the two-body problem. To provide an intuitive physical picture of our results, in Sec. III we summarize the physics of a pair of particles in a periodic lattice with power-law hopping. Subsequently, in Sec. IV we numerically demonstrate the extended-localized transition and calculate localization properties for both attractively and repulsively dimers. Finally, in Sec. V, we summarize and conclude the paper.

## II. GREEN'S FUNCTION FORMALISM

We consider a pair of interacting particles moving in a one-dimensional quasicrystal with power-law hopping. The Hamiltonian of the two-body system can be written as  $\hat{H} = \hat{H}_0 + \hat{U}$ , with  $\hat{H}_0$  the noninteracting component and  $\hat{U}$  the interaction operator. The ideal part of  $\hat{H}$  can be decomposed as  $\hat{H}_0 = \hat{H}_{\text{GAA}} \otimes \mathbb{I}_1 + \mathbb{I}_1 \otimes \hat{H}_{\text{GAA}}$ ,  $\mathbb{I}_1$  being the one-body identity operator and  $\hat{H}_{\text{GAA}}$  the single-particle generalized Aubry-André (GAA) Hamiltonian:

$$\hat{H}_{\text{GAA}} = -J \sum_{i,j \neq i} \frac{1}{|i-j|^\alpha} |i\rangle\langle j| + \Delta \sum_j \cos(2\pi\beta j + \phi) |j\rangle\langle j|, \quad (1)$$

where  $|j\rangle$  stands for the state in which the particle is localized at the site  $j$ , and  $J/|i-j|^\alpha$  is the hopping rate between the sites  $i$  and  $j$ . The quasiperiodic modulation is characterized by its strength  $\Delta$ , the incommensurate parameter  $\beta = (\sqrt{5} - 1)/2$ , and a random phase  $\phi \in [0, 2\pi)$ . For  $\alpha \gg 1$ , the GAA model approaches to the celebrated AA model [1,12,13,68]. As it is well known, all the eigenstates of the Aubry-André Hamiltonian are extended for  $\Delta/J < 2$ , all are localized for  $\Delta/J > 2$ , and all are multifractal at the transition point  $\Delta/J = 2$  [69]. In contrast, the GAA model displays a plethora of mobility edges that split extended and localized single-particle states for  $\alpha > 1$  [25], whereas for long-range hops  $\alpha < 1$  the single-particle states are extended or multifractal [25,26]. The operator  $\hat{U}$  couples the two particles by an on-site interaction of strength  $U$ :

$$\hat{U} = U \sum_j |j, j\rangle\langle j, j|, \quad (2)$$

$|j, j\rangle = |j\rangle \otimes |j\rangle$  being the two-body state in which both particles are in the lattice site  $j$ . It is important to mention

that the on-site interaction in Eq. (2) plays a role in spatially symmetric wave functions, where the particles can be found on the same site with nonzero probability. Thus, our results are relevant when the particles are bosons or fermions with opposite spins in the singlet state. The Schrödinger equation for the two-particle state  $|\Psi\rangle$  can be written as  $(E - \hat{H}_0)|\Psi\rangle = \hat{U}|\Psi\rangle$  with  $E$  the energy. This equation can be numerically solved with the aid of the noninteracting two-body Green's function operator  $\hat{G}_0(E) = (E - \hat{H}_0)^{-1}$ , which can be formally written in terms of the eigenstates  $|\varphi_l\rangle$  and eigenenergies  $\varepsilon_l$  of the GAA Hamiltonian:

$$\hat{G}_0(E) = \sum_{n,m} \frac{1}{E - \varepsilon_n - \varepsilon_m} |\varphi_n, \varphi_m\rangle\langle \varphi_n, \varphi_m|. \quad (3)$$

By applying  $\hat{G}_0$  to both sides of the Schrödinger equation  $(E - \hat{H}_0)|\Psi\rangle = \hat{U}|\Psi\rangle$ , one can find  $|\Psi\rangle = \hat{G}_0\hat{U}|\Psi\rangle$ . Projecting this last expression over the state  $|j, j'\rangle$ , we obtain an equation for the amplitudes  $\Psi(j, j') = \langle j, j'|\Psi\rangle$  of the two-particle wave function:

$$\begin{aligned} \Psi(j, j') &= \langle j, j'|\hat{G}_0\hat{U}|\Psi\rangle \\ &= U \sum_i \langle j, j'|\hat{G}_0(E)|i, i\rangle \Psi(i, i), \end{aligned} \quad (4)$$

where in the last equality we use the fact that the interaction operator  $\hat{U}$  is diagonal in the space representation. Equation (4) shows that  $\Psi(j, j')$  is entirely determined by its diagonal components  $\Psi(j, j)$  which, for simplicity, we shall denote by  $\psi(j) = \Psi(j, j)$ . Setting  $j = j'$  in Eq. (4) yields the desired eigenvalue problem:

$$\frac{1}{U} \psi(j) = \sum_i G_0(j, i; E) \psi(i), \quad (5)$$

$G_0(j, i; E)$  being the matrix elements of the noninteracting two-body Green's function operator:

$$\begin{aligned} G_0(j, i; E) &= \langle j, j|\hat{G}_0(E)|i, i\rangle \\ &= \sum_{n,m} \frac{\varphi_n(j)\varphi_m(j)\varphi_n^*(i)\varphi_m^*(i)}{E - \varepsilon_n - \varepsilon_m}. \end{aligned} \quad (6)$$

The computational complexity of the above equation is  $O(L^4)$  and, in contrast with tight-binding lattices, it cannot be reduced to  $O(L^3)$  since  $\hat{H}_{\text{GAA}}$  does not have a tridiagonal structure. For this reason, we restrict our calculations to a moderate lattice size of  $L = 377$ . In the Appendix, we perform a concise analysis of the relevance of the system size. Since the dimer motion is confined to one dimension, the bound state exists for arbitrarily small interactions. Furthermore, the eigenvalue problem in Eq. (5) admits solutions for negative and positive interaction strengths. The former states are called attractively bound pairs and the latter are called repulsively bound pairs. To solve for the attractively (repulsively) bound dimers, one starts by computing the matrix  $G_0(E)$  with an ansatz for the energy  $E$ , which is smaller (larger) than twice the lowest (highest) single-particle energy  $E < 2\varepsilon_1$  ( $E > 2\varepsilon_L$ ). Afterwards, one obtains the lowest (highest) eigenvalue of  $G_0(E)$  and compares it with  $1/U$ : If these values match, the lowest (highest) eigenvector of  $G_0(E)$  is the desired state; otherwise, the energy  $E$  must be varied until the lowest (highest) eigenvalue of the matrix  $G_0(E)$  equals  $1/U$ .

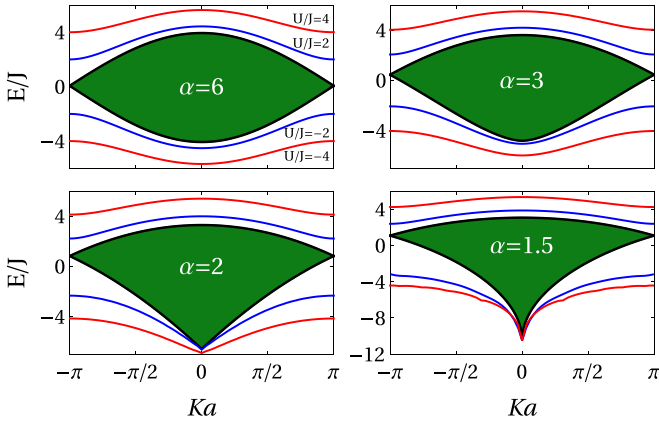


FIG. 1. Two-particle energies vs the center-of-mass momentum. The continuum (scattering) spectrum corresponds to the energies in green color. The lines above and below the scattering band are the energies of the repulsively and the attractively bound dimer, respectively.

In contrast to dimers bounded by an attractive interaction, a repulsively bound pair is not the ground state of the two-body system. However, due to energy constraints, the repulsively bound dimer is unable to decay by converting the interaction energy into kinetic energy and is therefore dynamically stable. In this paper, we concentrate on the minimal and maximal energy states of  $G_0(E)$ ; in the absence of quasiperiodic modulation, these states correspond to a pair of particles with zero center-of-mass momentum. To avoid any inconvenience with the thermodynamic limit of the pair energy, throughout the paper we shall consider  $\alpha > 1$  only.

### III. PERIODIC LATTICE

To provide an intuitive picture of the physics behind the asymmetry in the localized transition, in this section, we summarize the main characteristics of a pair of particles in a periodic lattice with power-law hopping. In the absence of quasiperiodicity  $\Delta/J = 0$ , the two-body wave function can be separated as  $\Psi(i, j) = e^{iKR} \Phi_K(r)$ , where  $R = (i + j)/2$  and  $r = |i - j|$  are the center-of-mass and relative coordinates, respectively. The relative coordinate wave function  $\Phi_K(r)$  depends on the center-of-mass momentum  $K \in [-\pi/a, \pi/a]$  with  $a$  the lattice constant. Using this ansatz, the eigenvalue problem in Eq. (5) reduces to  $G_{0,K}(E, 0)U = 1$ , where

$$G_{0,K}(E, r) = \frac{a}{2\pi} \int_{-\pi/a}^{\pi/a} dq \frac{e^{iqr}}{E - E_{Kq}} \quad (7)$$

is the noninteracting two-body Green's function and  $E_{Kq}$  is the two-particle dispersion relation, which is given as follows:

$$E_{Kq} = -J[\text{Li}_\alpha(e^{i(K/2+q)a}) + \text{Li}_\alpha(e^{-i(K/2+q)a}) + \text{Li}_\alpha(e^{i(K/2-q)a}) + \text{Li}_\alpha(e^{-i(K/2-q)a})], \quad (8)$$

$\text{Li}_\alpha(z)$  being the polylogarithm function and  $q$  the relative momentum. In Fig. 1, we show the two-particle energies as a function of the center-of-mass momentum for different power-law hops. Scattering energies are colored green whereas bound pair energies are above and below the scatter-

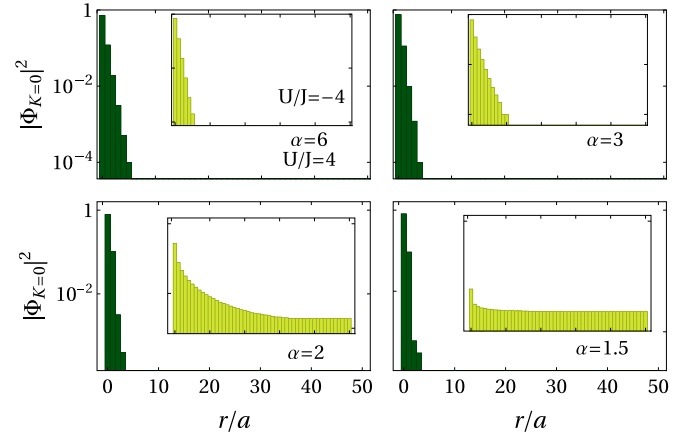


FIG. 2. Square modulus of the zero center-of-mass momentum wave function  $\Phi_{K=0}(r)$  vs the relative distance  $r$ . Main panels correspond to repulsively bound dimers with  $U/J = 4$ , whereas insets are associated with attractively bound pairs with  $U/J = -4$ .

ing band. As one can notice, the spectrum for  $\alpha = 6$  resembles the nearest-neighbor case, where if there is a state with energy  $E$  there is also a two-particle state with energy  $-E$ . However, as the range of the hopping increases ( $\alpha = 2$  and  $1.5$ ), the spectrum shows a clear asymmetry in both the scattering and dimer states. Up to a normalization factor, the relative wave function results proportional to the Green's function, that is,  $\Phi_K(r) \propto G_{0,K}(E, r)$ . In Fig. 2, we illustrate the square modulus of  $\Phi_{K=0}$  as a function of the relative coordinate  $r$  for several power-law hops. As one can notice, the spatial extent of  $\Phi_{K=0}$  for  $\alpha = 6$  is practically the same for repulsive and attractive interactions. However, for  $\alpha = 3, 1$ , and  $1/2$ , the relative wave function of the attractively bound dimers is delocalized in comparison with the wave function of the repulsively bound pairs. Due to the contrasting spatial behavior of repulsively and attractively bound dimers for  $\alpha = 3, 1$ , and  $1/2$ , one might intuitively expect that attractively bound dimers require larger quasiperiodic strengths than repulsively bound pairs to localize in space.

### IV. QUASIPERIODIC CHAIN

#### A. Extended-localized transition

In one-dimensional quasicrystals with nearest-neighbor tunneling, the wave function of a repulsively bound state with energy  $E$  describes also an attractively bound state with energy  $-E$ , provided the phase  $\phi$ , belonging to the AA potential, is shifted by  $\pi$ . In other words, while the attractively bound state localizes at the minimum of the quasiperiodic modulation, the repulsively bound state gets localized at the maximum. The fact that the same spatial profile represents both kinds of pairs implies that the two-body extended-localized transition does not depend on the interaction sign [50]. That is, the critical quasiperiodicity  $\Delta_c$  at which the transition takes place is an even function of the interaction strength  $\Delta_c(-U) = \Delta_c(U)$ . This is no longer true for one-dimensional quasicrystals with power-law hops; as illustrated in Fig. 3 (notice the log scale on the vertical axis), the diagonal elements of the two-body wave functions can show

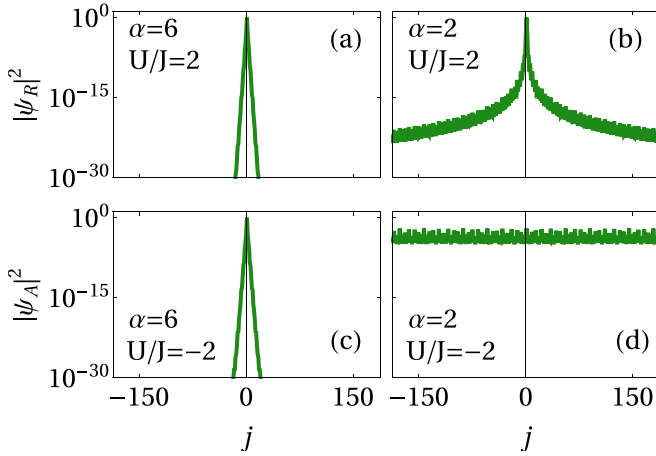


FIG. 3. Diagonal elements of the two-body profile  $\psi(j) = \Psi(j, j)$  as a function of the lattice index  $j$ ;  $\psi_A$  and  $\psi_R$  correspond to attractively and repulsively bound pairs, respectively. The strength of the quasiperiodic modulation for all panels is  $\Delta/J = 2$ .

contrasting spatial behaviors. In particular, while the attractively bound pair is extended for  $\alpha = 2$  and  $(U/J, \Delta/J) = (-2, 2)$ , the associated repulsively bound state for  $U/J = 2$  is localized. For  $\alpha = 6$ , the pair states are nearly identical, as expected from quasicrystals with short-range hops. The localized wave functions plotted in Fig. 3 correspond to phases  $\phi$  suitably chosen so that the site at which localization occurs coincides with the center of the lattice.

A customary parameter that is used as a measure of localization is the inverse participation ratio (IPR); given a normalized wave function  $\psi$  its IPR is defined as  $\text{IPR}_\psi = \sum_{i=1}^L |\psi(i)|^4$ . For extended states, the IPR vanishes in the thermodynamic limit as  $\propto L^{-1}$ , whereas for spatial localized profiles it is always finite. In Fig. 4, we plot in a density color scheme the inverse participation ratio of attractively and repulsively bound dimers as a function of  $\alpha$  and  $\Delta/J$  for several interaction strengths. The noninteracting cases shown

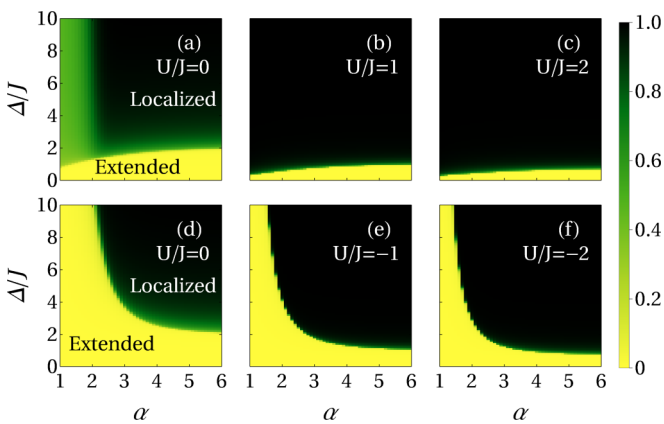


FIG. 4. Inverse participation ratio as a function of the power hop  $\alpha$  and the quasiperiodicity  $\Delta/J$  for several interaction strengths. The noninteracting cases in panels (a) and (d) are associated with the maximal and minimal energy states of the scattering band, respectively. All the calculations were obtained from the average of 30 random uniformly distributed phases  $\phi \in [0, 2\pi)$ .

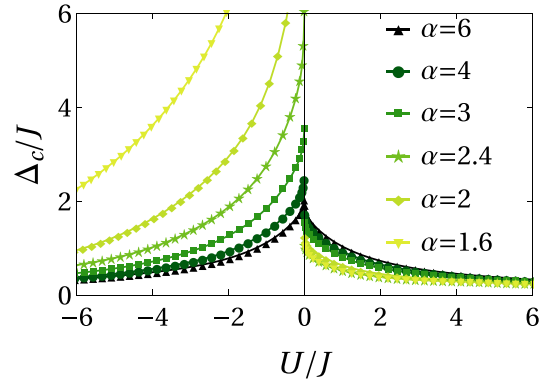


FIG. 5. Critical quasiperiodicity of the two-body extended-localized transition as a function of the interaction strength for several power-law hops. All the calculations were obtained from the average of 30 random uniformly distributed phases  $\phi \in [0, 2\pi)$ .

in Figs. 4(a) and 4(d) correspond to the maximal and minimal energy states of the scattering band, respectively. As one can notice, the interaction between particles favors the localization of both kinds of pairs. However, the IPR shows distinct features for attractive and repulsive interactions. For instance, as long as  $\alpha \lesssim 2$  attractively bound dimers are extended for large quasiperiodic modulations  $\Delta/J \approx 8$ . In contrast, all repulsively bound states are localized for these parameters. It is interesting to note that for attractively bound pairs the extended region, where the IPR is null, enlarges as  $\alpha$  decreases. In contrast, the extended region for repulsively bound dimers enlarges as  $\alpha$  increases.

To determine the critical quasiperiodicity  $\Delta_c/J$  at which the localization transition of the pairs takes place, we employ the inflection point technique of the inverse participation ratio. That is, for fixed values of  $U$  and  $\alpha$ , we calculate the IPR of the dimer state  $\psi$  as a function of  $\Delta$ , then we find the point where the second derivative of the obtained curve  $\text{IPR}(\Delta)$  vanishes. The inflection point technique has been successfully used in several previous works [50,56]. In addition, we compute the critical quasiperiodicity using the crossing point of the IPR and the normalized participation ratio,  $\text{NPR} = L^{-1}(\sum_{i=1}^L |\psi(i)|^4)^{-1}$ . We found that the deviations in  $\Delta_c/J$  obtained with both methods are less than 0.05J.

In Fig. 5 we illustrate the critical quasiperiodicity  $\Delta_c/J$  of the dimer localization transition as a function of the interaction strength  $U/J$  for several values of the power hop  $\alpha$ . For  $\alpha = 6$ , the critical quasiperiodic modulation is approximately an even function of the interaction strength, in agreement with quasicrystals with short-range hops [50]. As  $\alpha$  decreases, the mirror symmetry of  $\Delta_c/J$  with respect to  $U/J$  is completely broken, namely,  $\Delta_c(-U) \neq \Delta_c(U)$ . In particular, attractively bound dimers get localized at larger quasiperiodic modulations than repulsively bound states. Intuitively, one can forecast the previous assertion from the spatial behavior of repulsively and attractively dimers in the absence of quasiperiodic modulation (see Sec. III). To analyze the behavior of the two-body localization transition with respect to the range of the hopping, in Fig. 6, we illustrate the behavior of  $\Delta_c/J$  as a function of  $\alpha$  for several values of the interaction strength. Notice that the critical quasiperiodicity for repulsively bound

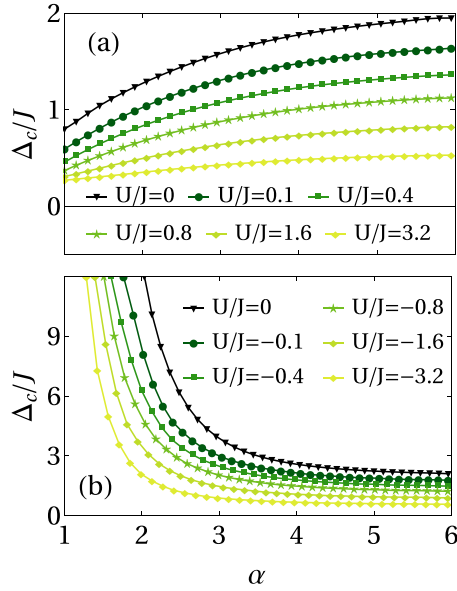


FIG. 6. Critical quasiperiodicity  $\Delta_c/J$  as a function of the hopping range  $\alpha$  for several interaction strengths  $U/J$ . Panels (a) and (b) correspond to repulsively and attractively bound dimers, respectively. All the calculations were obtained from the average of 30 random uniformly distributed phases  $\phi \in [0, 2\pi)$ .

pairs is always bounded by the Aubry-André transition point  $\Delta_c/J = 2$ . In contrast, for attractive interactions,  $\Delta_c/J$  exceeds the AA bound when the range of the hopping increases.

To provide a physical description of the two-particle system within the strongly interacting regime  $|U| \gg J, \Delta$ , we introduce an effective Hamiltonian  $\hat{H}_{\text{eff}}$  that describes tightly bound pairs. In this regime, the noninteracting component  $\hat{H}_0$  of the Hamiltonian  $\hat{H} = \hat{H}_0 + \hat{U}$  can be treated as a perturbation. To this end, we consider the operator  $\hat{P} = \sum_j |j, j\rangle\langle j, j|$  that projects over the states in which both particles are in the lattice site  $j$ . Then, the following effective Hamiltonian  $H_{\text{eff}}$  is obtained:

$$\hat{H}_{\text{eff}} = \hat{P}(\hat{U} + \hat{H}_0)\hat{P} + \hat{P}\hat{H}_0\hat{Q} \frac{1}{U - \hat{Q}\hat{U}\hat{Q}} \hat{Q}\hat{H}_0\hat{P}, \quad (9)$$

where  $\hat{Q} = \mathbb{I} - \hat{P}$ . After some straightforward algebra, one can write the effective Hamiltonian as  $\hat{H}_{\text{eff}} = \hat{T}_{\text{eff}} + \hat{V}_{\text{eff}}$ , where the effective mobility and on-site potential of the tightly bound dimer are given as follows:

$$\begin{aligned} \hat{T}_{\text{eff}} &= \frac{2J^2}{U} \sum_{i,j \neq i} \frac{1}{|i-j|^{2\alpha}} |i, i\rangle\langle j, j|, \\ \hat{V}_{\text{eff}} &= 2\Delta \sum_i \cos(2\pi\beta i + \phi) |i, i\rangle\langle i, i| \\ &\quad + \frac{4\Delta^2}{U} \sum_i \cos^2(2\pi\beta i + \phi) |i, i\rangle\langle i, i|. \end{aligned} \quad (10)$$

One can notice that the effective mobility of the dimer follows a power law  $1/r^\sigma$ , with  $\sigma = 2\alpha$ , namely, it is of shorter range than the hops of individual particles. As shown in Fig. 7, for tightly bound pairs  $\Delta_c \ll 1$ , hence one can safely neglect the  $\Delta^2$  term in Eq. (10); as a consequence, for sufficiently

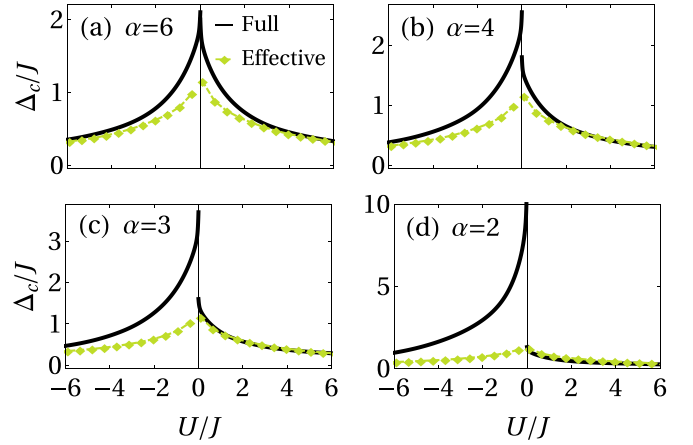


FIG. 7. Critical quasiperiodicity  $\Delta_c/J$  as a function of the interaction strength  $U/J$  for several power hops  $\alpha$ . The solid line corresponds to the full two-body prediction, whereas the dashed line with markers is associated with the effective Hamiltonian  $\hat{H}_{\text{eff}}$ .

large  $\alpha$ , the critical quasiperiodicity follows  $\Delta_c \approx 2/|U|$ , in agreement with quasicrystals with nearest-neighbor hoppings [50]. In Fig. 7, we compare the critical quasiperiodicity obtained by solving the full two-body problem [see Eq. (5)] with that estimated by the effective Hamiltonian [see Eq. (10)]. One can notice that for  $\alpha = 6$  the effective Hamiltonian gives an accurate prediction of the critical quasiperiodicity for  $|U|/J \gtrsim 4$ . However, when the range of the hopping increases, the accuracy of the effective model is highly dependent on the interaction sign. In particular,  $\hat{H}_{\text{eff}}$  begins to be a suitable description of the attractively bound dimer for larger interaction strengths than for the repulsively bound pair. As one can notice from Fig. 7(d), the effective model poorly describes the attractive branch whereas it gives reasonable predictions for  $U/J > 0$ .

## B. The pair energy gap

As it is well known, the total energy of repulsively and attractively bound pairs lies above and below the two-body scattering energies, respectively. The energy gap  $E_G$  between a bound state and the closest scattering state is a measure of the required energy to dissociate the pair. We should mention that the pair energy gap can be measured experimentally in optical lattices using rf spectroscopy [70,71]. Mathematically,  $E_G$  is defined as follows:

$$\begin{aligned} E_G^R &= E - 2\varepsilon_L, \\ E_G^A &= 2\varepsilon_1 - E, \end{aligned} \quad (11)$$

where the superscripts  $R$  and  $A$  are associated with repulsively and attractively bound dimers, respectively;  $\varepsilon_1$  is the lowest energy; and  $\varepsilon_L$  is the highest energy of the single-particle spectrum. In Figs. 8(a)–8(d), we show the pair energy gap  $E_G$  as a function of the interaction strength for  $\Delta/J = 0, 1, 2$ , and 3, respectively. The values of the hopping power  $\alpha$  are indicated in different colors. As illustrated in Fig. 8(a),  $E_G^R$  corresponds to positive  $U$ , while  $E_G^A$  is associated with negative interactions. For the periodic lattice  $\Delta/J = 0$ , one can see a very nearly mirror image between  $E_G^A$  and  $E_G^R$  when  $\alpha = 6$ .

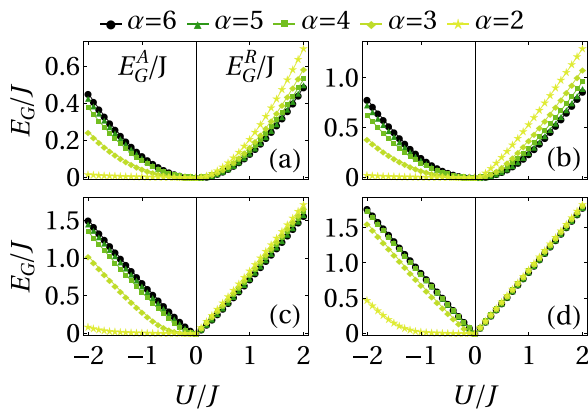


FIG. 8. The pair energy gap as a function of the interaction strength  $U$  for several values of the power-law hopping  $\alpha$ .  $E_G^A$  and  $E_G^R$  correspond to the attractive and repulsive branches, respectively. Panels (a), (b), (c), and (d) are associated with a quasiperiodic strength of  $\Delta/J = 0, 1, 2$ , and  $3$ , respectively.

However, as  $\alpha$  decreases, the asymmetric behavior of the pair energy gap is clearly seen. In particular, repulsively bound states exhibit a larger  $E_G$  than attractively bound pairs. As shown in Sec. III, similar asymmetric behavior is found in the absence of the quasiperiodic modulation. Because localized profiles increase the interaction energy, one can recognize from Figs. 8(b)–8(d) that the pair energy gap for both kinds of dimers increases significantly when the quasiperiodic potential localizes the two-particle wave function. Furthermore,

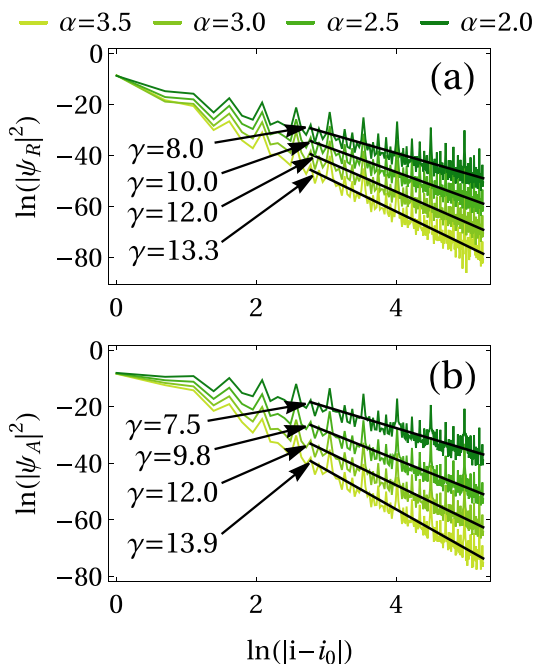


FIG. 9. Logarithm of  $|\psi|^2$  vs logarithm of the distance  $i$  from the localization center  $i_0$ . The arrows indicate the decay power  $|\psi|^2 \sim |i - i_0|^{-\gamma}$  of each wave function;  $\psi_A$  and  $\psi_R$  correspond to attractively and repulsively bound dimers, respectively. The parameters are  $(U/J, \Delta/J) = (3, 4)$  for panel (a), whereas panel (b) is associated with  $(U/J, \Delta/J) = (-3, 4)$ .

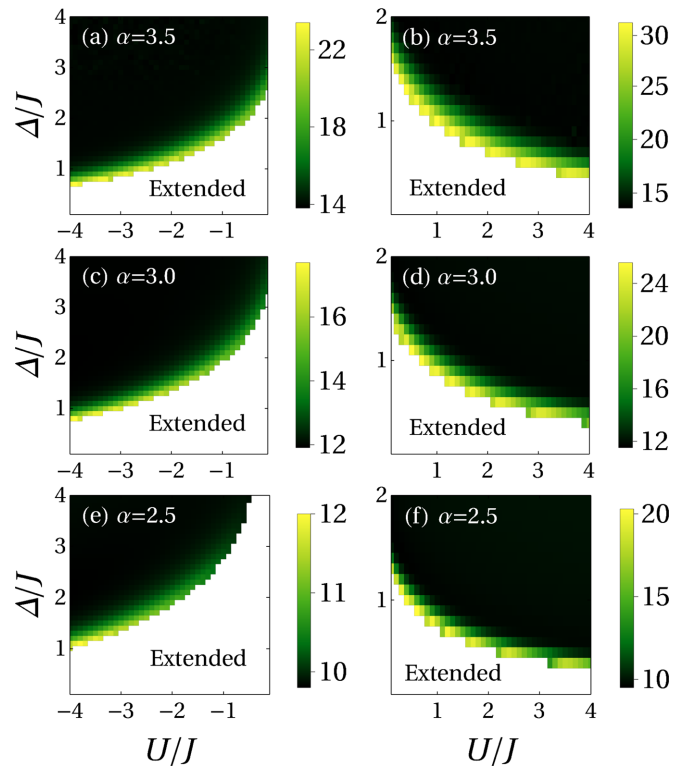


FIG. 10. Decay power  $\gamma$  as a function of interaction  $U/J$  and quasiperiodicity  $\Delta/J$  for three different power-law hops. All the calculations were obtained from the average of 30 random uniformly distributed phases  $\phi \in [0, 2\pi)$ .

due to a strong localization, the mobility of the pair ceases to play a relevant role, and therefore the curves associated with different values of  $\alpha$  gradually collapse to a straight line.

### C. Algebraic localization

As it is well known, localization in quasicrystals with nearest-neighbor hopping is characterized by exponential tails  $|\psi(i)|^2 \sim e^{-|i-i_0|/\xi}$ ,  $\xi$  being the localization length. In contrast, power-law tunneling yields algebraic decay  $|\psi(i)|^2 \sim |i - i_0|^{-\gamma}$ , where  $\gamma$  is the decay power and  $i_0$  is the localization center, which is placed at the maximum value of  $|\psi|^2$ . Recently, it has been found that algebraic single-particle states can be either conducting or insulating in the thermodynamic limit [72]. As illustrated in Fig. 9, the spatial distribution of attractively and repulsively dimers is well fitted by the algebraic dependence  $|i - i_0|^{-\gamma}$ ; the arrows in each panel indicate the corresponding value of  $\gamma$ . As one would expect, the decay power for both kinds of pairs increases as the tunneling range of the particles decreases. That is,  $|\psi|^2$  falls off more abruptly in space when  $\alpha$  increases. It is important to comment that for  $\alpha \gtrsim 4$  we found that the algebraic ansatz fits the profile poorly because  $|\psi|^2$  gradually recovers its exponential tail.

To understand the values of  $\gamma$  shown in Fig. 9, one can employ the effective Hamiltonian and a perturbative argument. Since we are interested in describing a localized profile, it is thus natural to consider  $\hat{T}_{\text{eff}}$  as a perturbation and develop a perturbative series for the eigenstates  $|\psi\rangle$  of  $\hat{H}_{\text{eff}}$  in powers of

*J.* To first order, the Lippmann-Schwinger equation reads

$$|\psi_j\rangle = |j\rangle - J \sum_{j_1} \frac{1}{|j_1 - j|^{2\alpha}} \frac{|j_1\rangle}{E - V_{\text{eff}}(j_1)}, \quad (12)$$

thus the square modulus of the pair wave function decays as  $|\psi|^2 \propto |i - j|^{-4\alpha}$ , which gives reasonable predictions of the values of  $\gamma$  shown in Fig. 9. Figures 10(a)–10(f) show the value of the decay power  $\gamma$  as a function of  $\Delta_c/J$  and  $U/J$  for repulsively and attractively bound pairs with three different values of  $\alpha$ . As one can notice, deep in the localized regime  $\gamma$  is well described by the prediction of the effective Hamiltonian, that is,  $\gamma = 4\alpha$ . However, near the transition point, the decay power  $\gamma$  deviates considerably from the perturbative result. Interestingly, we find that close to  $\Delta_c$  the wave function of repulsively bound dimers decays faster in space than attractively bound states.

## V. CONCLUSION

We have investigated the localization properties of two interacting particles moving in a one-dimensional quasicrystal with an adjustable tunneling range. In the proposed model, two identical bosons or fermions with opposite spins are coupled via a short-range interaction and tunnel not just through nearest-neighbor sites, but across the whole lattice with hopping couplings that follow a power-law function  $1/r^\alpha$ . By using Green's function techniques and numerical exact diagonalization, we have found that, in stark contrast with pair localization in quasicrystals with nearest-neighbor hops [50], the extended-localized transition of the dimer strongly depends on whether the interaction is repulsive or attractive. That is, the mirror symmetry of the critical quasiperiodicity at which the transition takes place is broken. In particular, we showed that the critical quasiperiodic modulation for repulsively bound states is always bounded by the usual Aubry-André transition point, whereas attractively pairs localize at larger quasiperiodic strengths when the range of the hopping increases. Furthermore, we numerically demonstrated that as the hopping range is decreased the mirror symmetry of the critical quasiperiodic modulation is restored, in agreement with previous literature on quasicrystals with nearest-neighbor hops. An extensive set of numerical calculations allowed us to determine the effects of interactions, quasiperiodicity, and hopping range on both the pair energy gap as well as the algebraic localization of the two-body system.

We expect that our analysis will trigger further theoretical work in determining both the fate and effects of dimer formation in the transport properties of many-body systems with

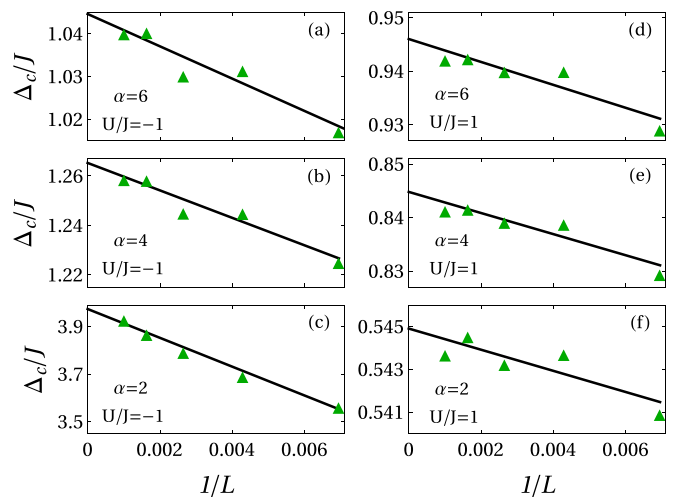


FIG. 11. Critical quasiperiodic strength  $\Delta_c/J$  as a function of the inverse lattice size  $1/L$  for  $L = 144, 233, 377, 610,$  and  $987$ . The solid black line in each panel corresponds to the infinite size  $1/L \rightarrow 0$  extrapolation.

power-law couplings. The model proposed in our paper is of current relevance for several quantum simulation platforms where power-law interactions emerge, for instance, trapped ions, Rydberg atoms, polar molecules, and atoms in photonic crystal waveguides among other systems.

## ACKNOWLEDGMENTS

This work was partially funded by Grant No. IN108620 from Dirección General de Asuntos del Personal Académico (DGAPA) (Universidad Nacional Autónoma de México). G.A.D.-C. acknowledges a Consejo Nacional de Ciencia y Tecnología (CONACYT) scholarship.

## APPENDIX: FINITE-SIZE SCALING

As mentioned in the paper, we have considered a lattice of size  $L = 377$ . However, it is particularly interesting to get an estimate of the relevance of the system size. For this reason, in this Appendix, as illustrated in Fig. 11 we show the critical quasiperiodic strength for several lattice sizes and the extrapolation of our finite size calculations to the infinite size.

As expected, finite-size errors are more noticeable as the hopping range increases. However, one can notice that  $L = 377$  gives reasonable predictions for the critical quasiperiodicity. Interestingly, repulsive interactions yield smaller finite-size errors than attractive interactions.

- [1] S. Aubry and G. André, *Ann. Israel Phys. Soc.* **3**, 133 (1980).
- [2] E. Maciá, *ISRN Condensed Matter Physics* **2014**, 165943 (2014).
- [3] X. Li, X. Li, and S. Das Sarma, *Phys. Rev. B* **96**, 085119 (2017).
- [4] M. Modugno, *New J. Phys.* **11**, 033023 (2009).
- [5] S. Roy, T. Mishra, B. Tanatar, and S. Basu, *Phys. Rev. Lett.* **126**, 106803 (2021).

- [6] A. Duthie, S. Roy, and D. E. Logan, *Phys. Rev. B* **103**, L060201 (2021).
- [7] X. Li and S. Das Sarma, *Phys. Rev. B* **101**, 064203 (2020).
- [8] H. Yao, A. Khoudli, L. Bresque, and L. Sanchez-Palencia, *Phys. Rev. Lett.* **123**, 070405 (2019).
- [9] G. Roati, C. D'Errico, L. Fallani, M. Fattori, C. Fort, M. Zaccanti, G. Modugno, M. Modugno, and M. Inguscio, *Nature (London)* **453**, 895 (2008).

- [10] H. P. Lüschen, S. Scherg, T. Kohlert, M. Schreiber, P. Bordia, X. Li, S. Das Sarma, and I. Bloch, *Phys. Rev. Lett.* **120**, 160404 (2018).
- [11] Y. Lahini, R. Pugatch, F. Pozzi, M. Sorel, R. Morandotti, N. Davidson, and Y. Silberberg, *Phys. Rev. Lett.* **103**, 013901 (2009).
- [12] P. G. Harper, *Proc. Phys. Soc. A* **68**, 874 (1955).
- [13] M. Ya. Azbel, *Phys. Rev. Lett.* **43**, 1954 (1979).
- [14] G. A. Domínguez-Castro and R. Paredes, *Eur. J. Phys.* **40**, 045403 (2019).
- [15] N. Defenu, T. Donner, T. Macrì, G. Pagano, S. Ruffo, and A. Trombettoni, *arXiv:2109.01063* (2021).
- [16] L. De Marco, G. Valtolina, K. Matsuda, W. G. Tobias, J. P. Covey, and J. Ye, *Science* **363**, 853 (2019).
- [17] S. A. Moses, J. P. Covey, M. T. Miecnikowski, D. S. Jin, and J. Ye, *Nat. Phys.* **13**, 13 (2017).
- [18] B. Yan, S. A. Moses, B. Gadway, J. P. Covey, K. R. A. Hazzard, A. M. Rey, D. S. Jin, and J. Ye, *Nature (London)* **501**, 521 (2013).
- [19] A. Browaeys and T. Lahaye, *Nat. Phys.* **16**, 132 (2020).
- [20] H. Labuhn, D. Barredo, S. Ravets, S. de Léséleuc, T. Macrì, T. Lahaye, and A. Browaeys, *Nature (London)* **534**, 667 (2016).
- [21] R. Blatt and C. F. Roos, *Nat. Phys.* **8**, 277 (2012).
- [22] P. Jurcevic, B. P. Lanyon, P. Hauke, C. Hempel, P. Zoller, R. Blatt, and C. F. Roos, *Nature (London)* **511**, 202 (2014).
- [23] C. Monroe, W. C. Campbell, L.-M. Duan, Z.-X. Gong, A. V. Gorshkov, P. W. Hess, R. Islam, K. Kim, N. M. Linke, G. Pagano, P. Richerme, C. Senko, and N. Y. Yao, *Rev. Mod. Phys.* **93**, 025001 (2021).
- [24] C.-L. Hung, A. González-Tudela, J. I. Cirac, and H. J. Kimble, *Proc. Natl. Acad. Sci. USA* **113**, E4946 (2016).
- [25] X. Deng, S. Ray, S. Sinha, G. V. Shlyapnikov, and L. Santos, *Phys. Rev. Lett.* **123**, 025301 (2019).
- [26] N. Roy and A. Sharma, *Phys. Rev. B* **103**, 075124 (2021).
- [27] X. Deng, V. E. Kravtsov, G. V. Shlyapnikov, and L. Santos, *Phys. Rev. Lett.* **120**, 110602 (2018).
- [28] M. Yan, H.-Y. Hui, M. Rigol, and V. W. Scarola, *Phys. Rev. Lett.* **119**, 073002 (2017).
- [29] R. K. Panda, A. Scardicchio, M. Schulz, S. R. Taylor, and M. Žnidarič, *Europhysics Letters* **128**, 67003 (2019).
- [30] P. Sierant, D. Delande, and J. Zakrzewski, *Phys. Rev. Lett.* **124**, 186601 (2020).
- [31] P. Sierant, E. G. Lazo, M. Dalmonte, A. Scardicchio, and J. Zakrzewski, *Phys. Rev. Lett.* **127**, 126603 (2021).
- [32] P. Sierant and J. Zakrzewski, *Phys. Rev. B* **105**, 224203 (2022).
- [33] R. Modak and T. Nag, *Phys. Rev. Res.* **2**, 012074(R) (2020).
- [34] R. Modak and T. Nag, *Phys. Rev. E* **101**, 052108 (2020).
- [35] J. Šuntajs, J. Bonča, T. Prosen, and L. Vidmar, *Phys. Rev. E* **102**, 062144 (2020).
- [36] M. Kiefer-Emmanouilidis, R. Unanyan, M. Fleischhauer, and J. Sirker, *Phys. Rev. Lett.* **124**, 243601 (2020).
- [37] M. Kiefer-Emmanouilidis, R. Unanyan, M. Fleischhauer, and J. Sirker, *Phys. Rev. B* **103**, 024203 (2021).
- [38] R. Nandkishore and D. A. Huse, *Annu. Rev. Condens. Matter Phys.* **6**, 15 (2015).
- [39] G. Vidal, *Phys. Rev. Lett.* **93**, 040502 (2004).
- [40] S. Paeckel, T. Köhler, A. Swoboda, S. R. Manmana, U. Schollwöck, and C. Hubig, *Ann. Phys. (NY)* **411**, 167998 (2019).
- [41] J. Haegeman, J. I. Cirac, T. J. Osborne, I. Pižorn, H. Verschelde, and F. Verstraete, *Phys. Rev. Lett.* **107**, 070601 (2011).
- [42] J.-Y. Choi, S. Hild, J. Zeiher, P. Schauß, A. Rubio-Abadal, T. Yefsah, V. Khemani, D. A. Huse, I. Bloch, and C. Gross, *Science* **352**, 1547 (2016).
- [43] M. Schreiber, S. S. Hodgman, P. Bordia, H. P. Lüschen, M. H. Fischer, R. Vosk, E. Altman, U. Schneider, and I. Bloch, *Science* **349**, 842 (2015).
- [44] T. Kohlert, S. Scherg, X. Li, H. P. Lüschen, S. Das Sarma, I. Bloch, and M. Aidelsburger, *Phys. Rev. Lett.* **122**, 170403 (2019).
- [45] A. Rubio-Abadal, J.-y. Choi, J. Zeiher, S. Hollerith, J. Rui, I. Bloch, and C. Gross, *Phys. Rev. X* **9**, 041014 (2019).
- [46] D. L. Shepelyansky, *Phys. Rev. Lett.* **73**, 2607 (1994).
- [47] F. von Oppen, T. Wettig, and J. Müller, *Phys. Rev. Lett.* **76**, 491 (1996).
- [48] D. O. Krimer, R. Khomeriki, and S. Flach, *JETP Lett.* **94**, 406 (2011).
- [49] D. Thongjaomayum, A. Andreanov, T. Engl, and S. Flach, *Phys. Rev. B* **100**, 224203 (2019).
- [50] G. Dufour and G. Orso, *Phys. Rev. Lett.* **109**, 155306 (2012).
- [51] S. Flach, M. Ivanchenko, and R. Khomeriki, *Europhys. Lett.* **98**, 66002 (2012).
- [52] K. M. Frahm and D. L. Shepelyansky, *Eur. Phys. J. B* **88**, 337 (2015).
- [53] D. L. Shepelyansky, *Phys. Rev. B* **54**, 14896 (1996).
- [54] P. H. Song and D. Kim, *Phys. Rev. B* **56**, 12217 (1997).
- [55] P. Mujal, A. Polls, S. Pilati, and B. Juliá-Díaz, *Phys. Rev. A* **100**, 013603 (2019).
- [56] G. Liu, *Eur. Phys. J. B* **94**, 12 (2021).
- [57] C. Lee, A. Rai, C. Noh, and D. G. Angelakis, *Phys. Rev. A* **89**, 023823 (2014).
- [58] F. Stellin and G. Orso, *Phys. Rev. Res.* **2**, 033501 (2020).
- [59] F. Stellin and G. Orso, *Phys. Rev. B* **102**, 144201 (2020).
- [60] D. Thongjaomayum, S. Flach, and A. Andreanov, *Phys. Rev. B* **101**, 174201 (2020).
- [61] G. A. Domínguez-Castro and R. Paredes, *Phys. Rev. A* **104**, 033306 (2021).
- [62] F. Serwane, G. Zürn, T. Lompe, T. B. Ottenstein, A. N. Wenz, and S. Jochim, *Science* **332**, 336 (2011).
- [63] A. Bergschneider, V. M. Klinkhamer, J. H. Becher, R. Klemt, L. Palm, G. Zürn, S. Jochim, and P. M. Preiss, *Nat. Phys.* **15**, 640 (2019).
- [64] J. H. Becher, E. Sindici, R. Klemt, S. Jochim, A. J. Daley, and P. M. Preiss, *Phys. Rev. Lett.* **125**, 180402 (2020).
- [65] T. Macrì, L. Lepori, G. Pagano, M. Lewenstein, and L. Barbiero, *Phys. Rev. B* **104**, 214309 (2021).
- [66] W. Li, A. Dhar, X. Deng, K. Kasamatsu, L. Barbiero, and L. Santos, *Phys. Rev. Lett.* **124**, 010404 (2020).
- [67] W.-H. Li, A. Dhar, X. Deng, and L. Santos, *Phys. Rev. A* **103**, 043331 (2021).
- [68] A. M. García-García and E. Cuevas, *Phys. Rev. B* **79**, 073104 (2009).
- [69] M. Wilkinson, *Proc. R. Soc. A* **391**, 305 (1984).
- [70] A. T. Sommer, L. W. Cheuk, M. J. H. Ku, W. S. Bakr, and M. W. Zwierlein, *Phys. Rev. Lett.* **108**, 045302 (2012).
- [71] H. Moritz, T. Stöferle, K. Günter, M. Köhl, and T. Esslinger, *Phys. Rev. Lett.* **94**, 210401 (2005).
- [72] M. Saha, S. K. Maiti, and A. Purkayastha, *Phys. Rev. B* **100**, 174201 (2019).